

A trip into Image Processing with Maurizio

Silvia Tozza

Dept. of Mathematics, ALMA MATER STUDIORUM University of Bologna



ALMA MATER STUDIORUM
UNIVERSITÀ DI BOLOGNA

*Nonlinear partial differential equations: Theory, Numerics and Applications
in memory of Maurizio Falcone*

Rome, May 24, 2023



Master degree, March 2011



Defense of my PhD Thesis, January 2015



UNIVERSITY
of York



SAPIENZA
UNIVERSITÀ DI ROMA

iNSAM

Istituto Nazionale di Alta Matematica



UNIVERSITÀ DEGLI STUDI DI NAPOLI
FEDERICO II



Dept. of Mathematics, ALMA MATER STUDIORUM Università di Bologna



ALMA MATER STUDIORUM
UNIVERSITÀ DI BOLOGNA

Enjoying trips (April 2019, Toulouse-Cabrerets)



Enjoying dinners together



Working together always with a smile and fun



Outline

- Stationary Hamilton-Jacobi equations
 - ▶ Introduction to Photometric 3D Reconstruction
 - ▶ Orthographic Shape-from-Shading (SfS)
 - ▶ Orthographic Photometric-Stereo SfS
- Time dependent Hamilton-Jacobi equations
 - ▶ Image Segmentation via Level-Set equation
 - ▶ Adaptive filtered schemes
 - ▶ Numerical experiments

Introduction - Shape-from-X Problems

Goal: Reconstruction of the shape of an object starting from some kind of data.

	Geometric techniques	Photometric techniques
Single image	Structured light	Shape-from-shading (SfS)
	Shape-from-shadows	
	Shape-from-contours	
	Shape-from-texture	
	Shape-from-template	
Multi-images	Structure-from-motion	Photometric stereo (PS)
	Stereopsis	Shape-from-polarisation (SfP)
	Shape-from-silhouettes	
	Shape-from-focus	

- Geometric techniques aim at identifying and analysing features
- Photometric techniques aim at inverting a physics-based image formation model.



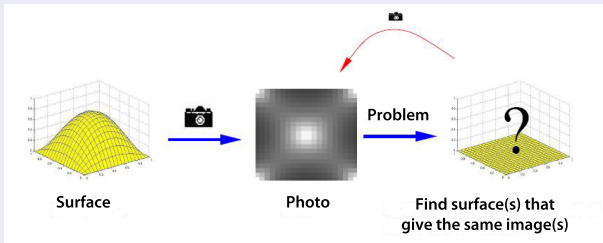
J.-D. Durou, M. Falcone, Y. Quéau, and **S. Tozza** (Eds.), *Advances in Photometric 3D-Reconstruction*, Advances in Computer Vision and Pattern Recognition, Springer 2020.

Introduction - Shape-from-X Problems

Goal: Reconstruction of the shape of an object starting from some kind of data.

Shape-from-Shading

Data: The gray-level measured in an image of the object



Introduction - Shape from Shading (SfS) Problem

Modeling of Shape from Shading:

- 1 Reflectance Model
- 2 Camera Model
- 3 Lighting Model

Orthographic SfS Problem

Modeling of Shape from Shading:

- 1 Reflectance Model
- 2 Camera Model \Rightarrow Orthographic Projection
- 3 Lighting Model \Rightarrow One light source located at infinity

Introduction - Shape from Shading (SfS) Problem

The SfS problem is described by the following irradiance equation:

$$R(\mathbf{N}(x, y)) = I(x, y) \quad (1)$$

where

- $R(\mathbf{N}(x, y))$ is the reflectance function
- $\mathbf{N}(x, y)$ is the unit normal to the surface at point $(x, y, u(x, y))$
- $I(x, y)$ is the graylevel measured in the image at point (x, y)

$I : \bar{\Omega} \rightarrow [0, 1]$, with $\bar{\Omega}$ compact domain ($\Omega \subset \mathbb{R}^2$ open subset).

Lambertian reflectance model (L-model)

Idea: The surface is Lambertian, i.e. the intensity reflected by a point of the surface is equal from all points of view.

Goal: Finding $u : \bar{\Omega} \rightarrow \mathbb{R}$ s. t. satisfies the following equation:

$$I(x, y) = \gamma_D \mathbf{N}(x, y) \cdot \boldsymbol{\omega}, \quad \forall (x, y) \in \Omega \quad (2)$$

where

- γ_D is the albedo
- $\mathbf{N}(x, y) = \frac{\mathbf{n}(x, y)}{|\mathbf{n}(x, y)|} = \frac{1}{\sqrt{1 + |\nabla u(x, y)|^2}} (-\nabla u(x, y), 1)$
- $\boldsymbol{\omega} = (\omega_1, \omega_2, \omega_3) = (\tilde{\boldsymbol{\omega}}, \omega_3)$ (general light direction)

Hamilton-Jacobi equation associated to (2):

$$I(x, y) \sqrt{1 + |\nabla u(x, y)|^2} + \tilde{\boldsymbol{\omega}} \cdot \nabla u(x, y) - \omega_3 = 0, \quad \text{in } \Omega.$$

Lambertian model: concave/convex ambiguity

Particular case: Vertical light source $\omega = (0, 0, 1)$

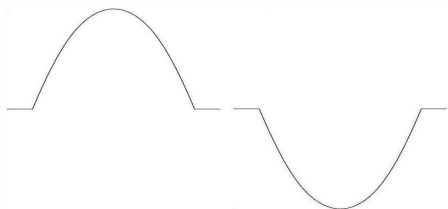
The HJ equation in the variable u becomes the so-called “eikonal equation”

$$|\nabla u(x, y)| = f(x, y) \quad \text{for } (x, y) \in \Omega, \quad (3)$$

where $f(x, y) = \sqrt{\frac{1}{I(x, y)^2} - 1}$.

Concave/convex ambiguity

The model is ill-posed, there is not uniqueness of solution (both in the context of classical and Lipschitz solutions).



Lambertian model: concave/convex ambiguity

Particular case: Vertical light source $\omega = (0, 0, 1)$

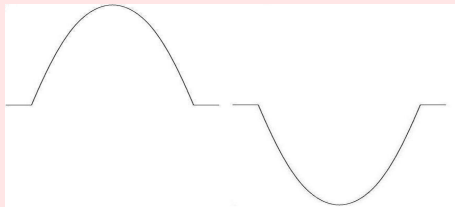
The HJ equation in the variable u becomes the so-called “eikonal equation”

$$|\nabla u(x, y)| = f(x, y) \quad \text{for } (x, y) \in \Omega, \quad (3)$$

where $f(x, y) = \sqrt{\frac{1}{I(x, y)^2} - 1}$.

Concave/convex ambiguity

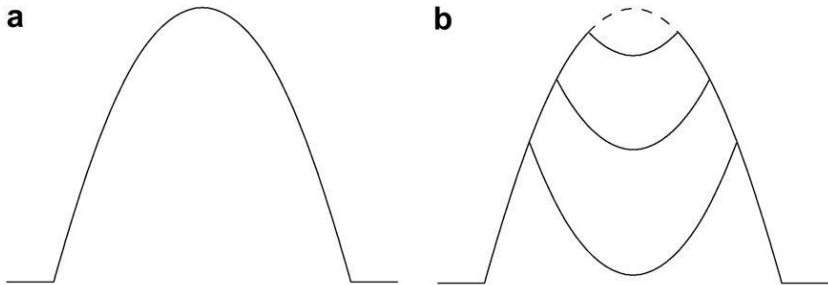
The model is ill-posed, there is not uniqueness of solution (both in the context of classical and Lipschitz solutions).



Lambertian model: concave/convex ambiguity

Concave/convex ambiguity: example

Eikonal equation (3) + Dirichlet BC zero



(a) maximal solution

and

(b) a.e. solutions that gives
the same image.

Lambertian model: concave/convex ambiguity

Possible solutions of the concave/convex problem:

- Fix the height value u at each point at maximum brightness (Lions-Rouy-Tourin, 1993)
- Choosing as a solution the maximal one, which is shown to be unique (Camilli-Siconolfi, 1999)
- Using more general reflectance model?

Non-Lambertian reflectance models do not solve the ambiguity for the orthographic SfS [T.-Falcone, JMIV 2016]



[S. Tozza](#), M. Falcone, Analysis and approximation of some Shape-from-Shading models for non-Lambertian surfaces, *JMIV*, 55(2):153-178, 2016.

Lambertian model: concave/convex ambiguity

Possible solutions of the concave/convex problem:

- Fix the height value u at each point at maximum brightness (Lions-Rouy-Tourin, 1993)
- Choosing as a solution the maximal one, which is shown to be unique (Camilli-Siconolfi, 1999)
- Using more general reflectance model?

Non-Lambertian reflectance models do not solve the ambiguity for the orthographic SfS [T.-Falcone, JMIV 2016]



[S. Tozza](#), M. Falcone, Analysis and approximation of some Shape-from-Shading models for non-Lambertian surfaces, *JMIV*, 55(2):153-178, 2016.

Lambertian model: concave/convex ambiguity

Possible solutions of the concave/convex problem:

- Fix the height value u at each point at maximum brightness (Lions-Rouy-Tourin, 1993)
- Choosing as a solution the maximal one, which is shown to be unique (Camilli-Siconolfi, 1999)
- Using more general reflectance model?

Non-Lambertian reflectance models do not solve the ambiguity for the orthographic SfS [T.-Falcone, JMIV 2016]



S. Tozza, M. Falcone, Analysis and approximation of some Shape-from-Shading models for non-Lambertian surfaces, *JMIV*, 55(2):153-178, 2016.

Lambertian model: concave/convex ambiguity

Possible solutions of the concave/convex problem:

- Fix the height value u at each point at maximum brightness (Lions-Rouy-Tourin, 1993)
- Choosing as a solution the maximal one, which is shown to be unique (Camilli-Siconolfi, 1999)
- Using more general reflectance model?

Non-Lambertian reflectance models do not solve the ambiguity for the orthographic SfS [T.-Falcone, JMIV 2016]



S. Tozza, M. Falcone, Analysis and approximation of some Shape-from-Shading models for non-Lambertian surfaces, *JMIV*, **55**(2):153-178, 2016.

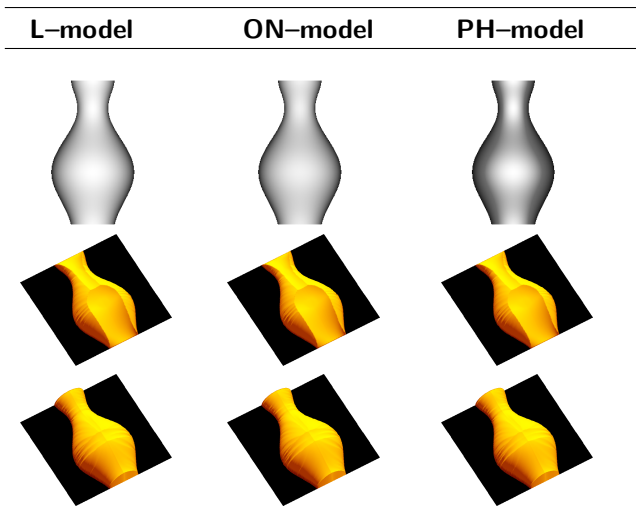


Figure: Synthetic vase under vertical light source ($\omega = (0, 0, 1)$): example of concave/convex ambiguity solved by using correct Dirichlet BC. From left to right: L-model, ON-model with $\sigma = 0.2$, PH-model with $k_S = 0.4$.

Well-posed Orthographic problem (L-model)

- Photometric Stereo SfS with two light sources plus Boundary Conditions

$$\begin{cases} \gamma_D(x, y) \frac{-\nabla u(x, y) \cdot \tilde{\omega}' + \omega'_3}{\sqrt{1 + \|\nabla u(x, y)\|^2}} = D_1(x, y), & \forall (x, y) \in \Omega \\ \gamma_D(x, y) \frac{-\nabla u(x, y) \cdot \tilde{\omega}'' + \omega''_3}{\sqrt{1 + \|\nabla u(x, y)\|^2}} = D_2(x, y), & \forall (x, y) \in \Omega \end{cases}$$

with $u(x, y) = g(x, y)$ known for all $(x, y) \in \partial\Omega$.

By eliminating the non-linearity we arrive to

$$\begin{cases} \mathbf{b}_D(x, y) \cdot \nabla u(x, y) = f_D(x, y), & \text{a.e. } (x, y) \in \Omega \\ u(x, y) = g(x, y), & \forall (x, y) \in \partial\Omega \end{cases} \quad (4)$$



R. Mecca and M. Falcone, Uniqueness and Approximation of a Photometric Shape-from-Shading Model, SIAM J. Imaging Sciences, 6(1):616-659, 2013

Standard PS-SfS

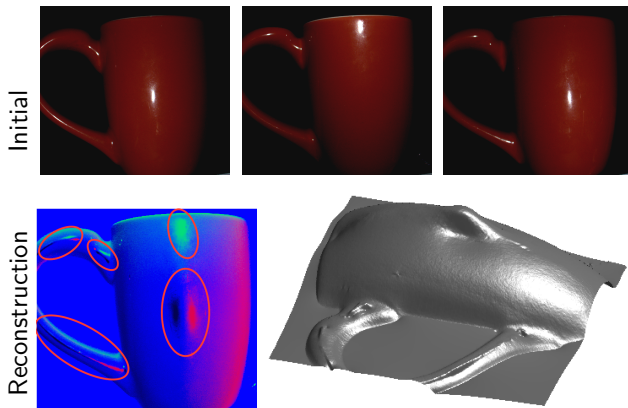
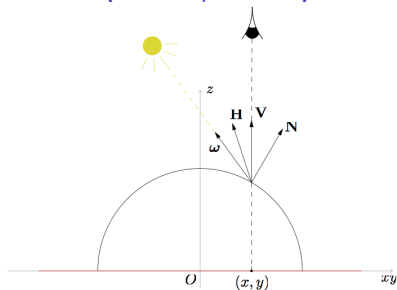
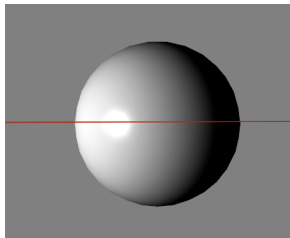


Figure: The top row shows three images of a painted ceramic cup. The bottom row shows the normal map where artifacts have been highlighted and the 3D shape reconstruction using traditional PS [R. J. Woodham (1980)]. Bottom images show artifacts due to specular reflections.

Specular model - Blinn-Phong model (Blinn, 1977)



The Blinn-Phong Specular model

$$S_i(x, y) = \gamma_S(x, y)(\mathbf{H}^i \cdot \mathbf{N}(x, y))^c$$

where

- $\gamma_S(x, y)$ is the specular albedo,
- $\mathbf{H}^i = \frac{\mathbf{V} + \boldsymbol{\omega}^i}{|\mathbf{V} + \boldsymbol{\omega}^i|} = \frac{\mathbf{h}^i}{|\mathbf{h}^i|} = \left(\frac{h_1^i}{|\mathbf{h}^i|}, \frac{h_2^i}{|\mathbf{h}^i|}, \frac{h_3^i}{|\mathbf{h}^i|} \right)$, ($V_3 > 0, \omega_3 > 0$)
- $c > 0$ measures the shininess of the surface.

Specular model - Blinn-Phong model

By using the technique of the image ratios:

$$\underbrace{\frac{\mathbf{n}(x, y) \cdot \mathbf{h}'}{|\mathbf{h}'|(S_1(x, y))^{\frac{1}{c}}}}_{\text{Equation for } S_1} = \overbrace{\frac{|\mathbf{n}(x, y)|}{(\gamma_S(x, y))^{\frac{1}{c}}} = \frac{\mathbf{n}(x, y) \cdot \mathbf{h}''}{|\mathbf{h}''|(S_2(x, y))^{\frac{1}{c}}}}_{\text{Equation for } S_2}$$

we arrive to the following

Specular Differential problem (Cf. with the diffuse one (4))

$$\begin{cases} \mathbf{b}_S(x, y) \cdot \nabla u(x, y) = f_S(x, y) & \text{a.e. } (x, y) \in \Omega, \\ u(x, y) = g(x, y) & \forall (x, y) \in \partial\Omega, \end{cases} \quad (5)$$

with the same boundary conditions and

$$(\mathbf{b}_S, f_S) = |\mathbf{h}''|(S_2(x, y))^{\frac{1}{c}} \mathbf{h}' - |\mathbf{h}'|(S_1(x, y))^{\frac{1}{c}} \mathbf{h}''.$$

Also the specular problem is albedo independent!

Well-posed Orthographic problem (L-model+BP-model)

We combine the diffuse and specular equations with a weight $\alpha(x, y) \in \{0, 1\}$ as follows:

$$\begin{cases} \mathbf{b}(x, y) \cdot \nabla u(x, y) = f(x, y) & \text{a.e. } (x, y) \in \Omega, \\ u(x, y) = g(x, y) & \forall (x, y) \in \partial\Omega, \end{cases} \quad (6)$$

where

$$\begin{aligned} \mathbf{b}(x, y) &= \alpha(x, y)\mathbf{b}_D(x, y) + (1 - \alpha(x, y))\mathbf{b}_S(x, y) \\ f(x, y) &= \alpha(x, y)f_D(x, y) + (1 - \alpha(x, y))f_S(x, y). \end{aligned}$$

α is a given coefficient, provided by the separation procedure between specular and diffuse components.

We show that the problem (6) is well-posed!



S. Tozza, R. Mecca, M. Duocastella, A. Del Bue, Direct Differential Photometric Stereo Shape Recovery of Diffuse and Specular Surfaces, *Journal of Mathematical Imaging and Vision*, **56**(1):57-76, 2016.

Numerical Examples [Tozza et al., JMIV 2016]

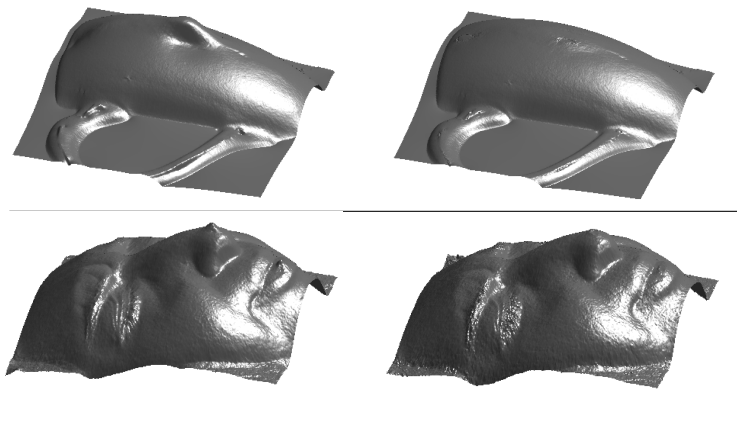


Figure: Reconstructions of a cup (top) and of a human face (bottom). From left to right: traditional PS approach with global diffuse reflection, our method.

Well-posed Orthographic problem (L-model)

Using three images (obtained by three not coplanar light sources) we can solve the PS-SfS problem without boundary conditions [Mecca-T., 2013] through the following system of hyperbolic equations:

$$\begin{cases} b^{(1,2)}(x, y) \cdot \nabla u(x, y) = f^{(1,2)}(x, y), & \text{a.e. } (x, y) \in \Omega \\ b^{(1,3)}(x, y) \cdot \nabla u(x, y) = f^{(1,3)}(x, y), & \text{a.e. } (x, y) \in \Omega \\ b^{(2,3)}(x, y) \cdot \nabla u(x, y) = f^{(2,3)}(x, y), & \text{a.e. } (x, y) \in \Omega \end{cases} \quad (7)$$

where

$$b^{(h,k)}(x, y) = (I_k(x, y)\omega_1^h - I_h(x, y)\omega_1^k, I_k(x, y)\omega_2^h - I_h(x, y)\omega_2^k)$$

and

$$f(x, y)^{(h,k)} = I_k(x, y)\omega_3^h - I_h(x, y)\omega_3^k$$

If the surface has some symmetries, we can solve the problem with 2 or only 1 input image.



R. Mecca and [S. Tozza](#), Shape Reconstruction of Symmetric Surfaces using Photometric Stereo, In: *Innovations for Shape Analysis: Models and Algorithms*, pp. 219-243, Springer Edition, 2013.

PS-SfS Numerical Scheme

Idea

Integrating the solution along the characteristics.

$$\nabla_{\rho(x,y)} u(x, y) = \frac{f(x, y)}{\|\mathbf{b}(x, y)\|}, \quad \forall (x, y) \in \Omega$$

with $\rho(x, y) = \frac{\mathbf{b}(x, y)}{\|\mathbf{b}(x, y)\|}$.

The following approximation holds:

$$\frac{u(x + h\rho_1(x, y), y + h\rho_2(x, y)) - u(x, y)}{h} \simeq \frac{f(x, y)}{\|\mathbf{b}(x, y)\|}, \quad \forall (x, y) \in \Omega.$$

from which we can derive

The backward Semi-Lagrangian (SL) Scheme

$$u_{i,j}^{n+1} = u^n(x_i + h\rho_1(x_i, y_j), y_j + h\rho_2(x_i, y_j)) - \frac{f_{i,j}}{\|\mathbf{b}_{i,j}\|} h, \quad \forall (x_i, y_j) \in \Omega_d.$$

Analogously, we can obtain the Forward SL Scheme.

PS-SfS Numerical Test: Real Beethoven


 I_1^{real}
 I_2^{real}
 I_3^{real}

Angles:

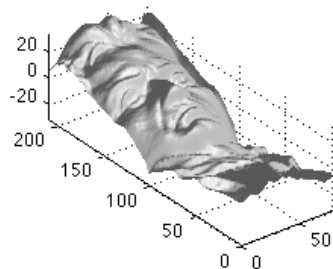
$$\theta_1 = -0.305, \varphi_1 = 0.263 \text{ per } I_1^{real};$$

$$\theta_2 = 3.226, \varphi_2 = 0.2 \text{ per } I_2^{real};$$

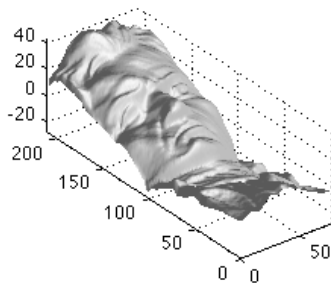
$$\theta_3 = 3.502, \varphi_3 = 0.281 \text{ per } I_3^{real}.$$

PS-SfS Numerical Test: Real Beethoven

Schema semi lagrangiano in avanti



Schema semi lagrangiano all'indietro



R. Mecca and [S. Tozza](#), Shape Reconstruction of Symmetric Surfaces using Photometric Stereo, In: *Innovations for Shape Analysis: Models and Algorithms*, pp. 219-243, Springer Edition, 2013.

Perspective SfS Problem

Modeling of Shape from Shading:

- 1 Reflectance Model
- 2 Camera Model \Rightarrow Perspective Projection
- 3 Lighting Model \Rightarrow One light source located at the optical center of the camera

\rightarrow Adding an attenuation term of the illumination due to the distance between the surface and the light source is possible to get well-posedness.



F. Camilli and [S. Tozza](#), A Unified Approach to the Well-Posedness of Some Non-Lambertian Models in Shape-from-Shading Theory, *SIAM J. Imaging Sci.*, 10:26–46, 2017.



[S. Tozza](#), Perspective Shape-from-Shading Problem: A Unified Convergence Result for Several Non-Lambertian Models, *J. Imaging*, 8, 36, 2022.

Perspective SfS Problem

Modeling of Shape from Shading:

- 1 Reflectance Model
- 2 Camera Model \Rightarrow Perspective Projection
- 3 Lighting Model \Rightarrow One light source located at the optical center of the camera

\rightarrow Adding an attenuation term of the illumination due to the distance between the surface and the light source is possible to get well-posedness.



F. Camilli and [S. Tozza](#), A Unified Approach to the Well-Posedness of Some Non-Lambertian Models in Shape-from-Shading Theory, *SIAM J. Imaging Sci.* , **10**:26–46, 2017.



[S. Tozza](#), Perspective Shape-from-Shading Problem: A Unified Convergence Result for Several Non-Lambertian Models, *J. Imaging*. **8**, 36, 2022.

From 3D Vision to 3D Printing

Springer INdAM Series

Giorgio Patrino *Editor-in-Chief*

Giovanni Alberici · Filippo Bracci · Claudia Carotto · Vincenzo Ferone · Claudio Fontanesi
 Giuseppina Muscatello · Angela Pizziti · Marco Sammartino *Series Editors*

Emiliano Cristiani · Maurizio Falcone · Silvia Tozza *Editors*

Mathematical Methods for Objects Reconstruction

From 3D Vision to 3D Printing

The volume collects several contributions to the INdAM workshop *Mathematical Methods for Objects Reconstruction: from 3D Vision to 3D Printing* held in Rome, February, 2021.

The goal of the workshop was to discuss new methods and conceptual structures for managing these challenging problems. The chapters reflect this goal and the authors are academic researchers and some experts from industry working in the areas of 3D modeling, computer vision, 3D printing and/or developing new mathematical methods for these problems. The contributions present methodologies and challenges raised by the emergence of large-scale 3D reconstruction applications and low-cost 3D printers. The volume collects complementary knowledges from different areas of mathematics, computer science and engineering on research topics related to 3D printing, which are, so far, widely unexplored.

Young researchers and future scientific leaders in the field of 3D data acquisition, 3D scene reconstruction, and 3D printing software development will find an excellent introduction to these problems and to the mathematical techniques necessary to solve them.

ISBN 978-981-99-0773-5



► springer.com

54
 Cristiani · Falcone
 Tozza *Eds.*

Springer INdAM Series 54

Emiliano Cristiani · Maurizio Falcone
 Silvia Tozza *Editors*



Mathematical Methods for Objects
 Reconstruction

Mathematical Methods for Objects Reconstruction

From 3D Vision to 3D Printing

Springer

Introduction - Evolutive Part

Time dependent HJ equation

We are interested in computing the approximation of viscosity solution of Hamilton-Jacobi (HJ) equation:

$$\begin{cases} \partial_t v + H(x, \nabla v) = 0, & (t, x) \in (0, T) \times \mathbb{R}^d, \\ v(0, x) = v_0(x), & x \in \mathbb{R}^d. \end{cases} \quad (8)$$

(H1) $H(x, p)$ is Lipschitz continuous w.r.t. all variables

(H2) $v_0(x)$ is Lipschitz continuous.

- Under these assumptions we have existence and uniqueness of the viscosity solution for (8).

Challenges and motivations

- In general, the solution is not classical ($v \in C^1$) and can develop singularities in finite time
- We need to have a good resolution of the solution even at kinks
- High-order schemes allow the use of coarser grids
- Few convergence results for high-order schemes in literature
- Several interesting applications: computer vision, optimal control, front propagation, differential games...

GOAL: Construct convergent schemes to the viscosity solution v of (8) with the property to be of high-order in the region of regularity.

Challenges and motivations

- In general, the solution is not classical ($v \in C^1$) and can develop singularities in finite time
- We need to have a good resolution of the solution even at kinks
- High-order schemes allow the use of coarser grids
- Few convergence results for high-order schemes in literature
- Several interesting applications: computer vision, optimal control, front propagation, differential games...

GOAL: Construct convergent schemes to the viscosity solution v of (8) with the property to be of high-order in the region of regularity.

The Level-Set (LS) equation (Sethian '85, '99, Osher-Sethian '88)

The model equation corresponding to the LS method is

$$\begin{cases} \partial_t v(t, x, y) + c(x, y)|\nabla v(t, x, y)| = 0, & (t, x, y) \in [0, T] \times \mathbb{R}^2, \\ v(0, x, y) = v_0(x, y), & (x, y) \in \mathbb{R}^2. \end{cases}$$

- The unknown is a "representation" function $v : [0, T] \times \mathbb{R}^2 \rightarrow \mathbb{R}$ of the interface
- The position of the interface Γ_t at time t is given by the 0-level set of $v(t, \cdot)$, i.e. $\Gamma_t = \{(x, y) : v(t, x, y) = 0\}$
- v_0 must be a representation function for the initial front $\partial\Omega_0$ where $\Omega_0 \subset \mathbb{R}^2$ is an open and bounded set, i.e.

$$\begin{cases} v_0(x, y) > 0 & \text{in } \Omega_0, \\ v_0(x, y) = 0 & \text{on } \partial\Omega_0 := \Gamma_0, \\ v_0(x, y) < 0 & \text{in } \mathbb{R}^2 \setminus \overline{\Omega_0}. \end{cases}$$

- $c(x, y)$ is the velocity of the front in the normal direction

$$\eta(t, x, y) = \frac{\nabla v(t, x, y)}{|\nabla v(t, x, y)|}.$$

The Level-Set (LS) equation

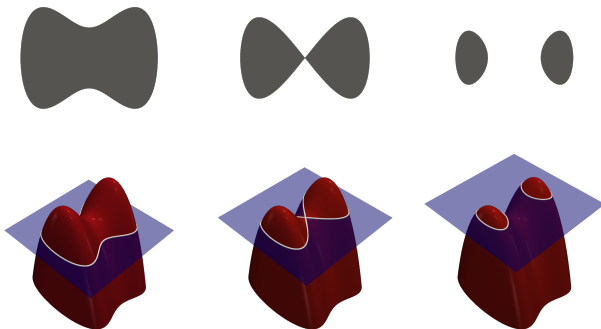


Figure: Illustration of the LS idea.

Image Segmentation problem

Goal

Detect the boundaries of objects represented in a picture.

A very popular method for segmentation is based on the level set method, this application is often called "Active contour" since the segmentation is obtained following the evolution of a simple curve (a circle for example) in its normal direction.

Key idea behind LS

The boundaries of a specific object inside a given image, described by the intensity function $I(x, y)$, are characterized by an abrupt change of the values of I , so that the magnitude of $|\nabla I|$ can be used as an indication of the edges.

In order to make use of this intuition, we have to define the velocity $c(x, y)$ accordingly.

Possible choices of the velocity function

Two different definitions proposed in Malladi-Sethian-Vemuri (1993):

$$c_1(x, y) = \frac{1}{(1 + |\nabla(G * I)|^\mu)}, \quad \mu \geq 1$$

$$c_2(x, y) = 1 - \frac{|\nabla(G * I(x, y))| - M_2}{M_1 - M_2},$$

where M_1 and M_2 are the maximum and minimum values of $|\nabla(G * I(x, y))|$.

Common properties

- Both velocities take values in $[0, 1]$
- close to 0 if there is a rapid change in the values of I (or if the magnitude of the image gradient is close to its maximal value).

Possible choices of the velocity function

Two different definitions proposed in Malladi-Sethian-Vemuri (1993):

$$c_1(x, y) = \frac{1}{(1 + |\nabla(G * I)|^\mu)}, \quad \mu \geq 1$$

$$c_2(x, y) = 1 - \frac{|\nabla(G * I(x, y))| - M_2}{M_1 - M_2},$$

where M_1 and M_2 are the maximum and minimum values of $|\nabla(G * I(x, y))|$.

Different features

- c_1 depends more heavily on the changes in the magnitude of the gradient.
⇒ Easier detection of the edges but can produce false edges inside the object (e.g. in presence of specularities).
- c_2 is smoother inside the objects, being less dependent on the relative changes in the gradient.
⇒ Possible problems in the detection of all the edges if at least one is "more marked".

Possible choices of the velocity function

Considering

$$v_0(x, y) = \text{dist}\{(x, y), \Gamma_0\}$$

then by construction all the C -level set are at a distance C from the 0-level set.

If we consider a generic point (x_c, y_c) on a C -level set, then it is reasonable to assume that the closest point on Γ_0 should be

$$(x_0, y_0) = (x_c, y_c) - v(t, x_c, y_c) \frac{\nabla v(t, x_c, y_c)}{|\nabla v(t, x_c, y_c)|}.$$

Possible choices of the velocity function

Therefore, it seems natural to define the **extended velocity** $\tilde{c}(x, y)$ as

$$\tilde{c}(x, y, v, v_x, v_y) = c\left(x - v \frac{v_x}{|\nabla v|}, y - v \frac{v_y}{|\nabla v|}\right), \quad (9)$$

which coincides with $c(x, y)$ on the 0-level set, as it is needed.

Since the idea behind the modification of the velocity $c(x, y)$ into \tilde{c} is to follow the evolution of the 0-level set and then to define accordingly the evolution on the other level sets, we can see the new definition, in some sense, *as a characteristic based velocity*.

Initial conditions: expansion and shrinking cases



Figure: Initial fronts for the two cases tested.

Filtered schemes

- We look for non-monotone schemes since we want to get a high-order scheme
- We want to find a convergent scheme that approximates the viscosity solution of (8)

We start from the results in Bokanowski, Falcone and Sahu (2016) and by Oberman and Salvador (2015) and we extend them introducing an adaptive choice of the parameter controlling the filter.

Adaptive Filtered Scheme

The proposed adaptive scheme is

$$u_{i,j}^{n+1} = S^{AF}(u^n)_{i,j} := S^M(u^n)_{i,j} + \phi_{i,j}^n \varepsilon^n \Delta t F \left(\frac{S^A(u^n)_{i,j} - S^M(u^n)_{i,j}}{\varepsilon^n \Delta t} \right), \quad (10)$$

starting from the initial condition $u_{i,j}^0$.

- $\varepsilon^n = \varepsilon^n(\Delta t, \Delta x, \Delta y) > 0$ is the *switching parameter* that will satisfy

$$\lim_{(\Delta t, \Delta x, \Delta y) \rightarrow 0} \varepsilon^n = 0$$

- $F : \mathbb{R} \rightarrow \mathbb{R}$ is the *filter function*
- $\phi_{i,j}^n$ is the *smoothness indicator function* at the node (x_j, y_i) and time t_n , based on the 2D-smoothness indicators defined in (Falcone-Paolucci-T., JCP, 2020).

Adaptive Filtered Scheme

The proposed adaptive scheme is

$$u_{i,j}^{n+1} = S^{AF}(u^n)_{i,j} := S^M(u^n)_{i,j} + \phi_{i,j}^n \varepsilon^n \Delta t F \left(\frac{S^A(u^n)_{i,j} - S^M(u^n)_{i,j}}{\varepsilon^n \Delta t} \right), \quad (10)$$

starting from the initial condition $u_{i,j}^0$.

- $\varepsilon^n = \varepsilon^n(\Delta t, \Delta x, \Delta y) > 0$ is the **switching parameter** that will satisfy

$$\lim_{(\Delta t, \Delta x, \Delta y) \rightarrow 0} \varepsilon^n = 0$$

- $F : \mathbb{R} \rightarrow \mathbb{R}$ is the **filter function**
- $\phi_{i,j}^n$ is the **smoothness indicator function** at the node (x_j, y_i) and time t_n , based on the 2D-smoothness indicators defined in (Falcone-Paolucci-T., JCP, 2020).

Assumptions on S^M

The scheme is consistent, monotone and can be written in *differenced form*

$$u_{i,j}^{n+1} = S^M(u^n)_{i,j} := u_{i,j}^n - \Delta t h^M(x_j, y_i, D_x^- u_{i,j}^n, D_x^+ u_{i,j}^n; D_y^- u_{i,j}^n, D_y^+ u_{i,j}^n)$$

for a Lipschitz continuous function $h^M(x, y, p^-, p^+; q^-, q^+)$, with

$$D_x^\pm u_{i,j}^n := \pm \frac{u_{i,j\pm 1}^n - u_{i,j}^n}{\Delta x} \quad \text{and} \quad D_y^\pm u_{i,j}^n := \pm \frac{u_{i\pm 1,j}^n - u_{i,j}^n}{\Delta y}.$$

Assumptions on S^A

S^A has a high-order consistency and can be written in *differenced form*

$$u_{i,j}^{n+1} = S^A(u^n)_{i,j} := u_{i,j}^n - \Delta t h^A(x_j, y_i, D_{k,x}^- u_{i,j}^n, \dots, D_x^- u_{i,j}^n, D_x^+ u_{i,j}^n, \dots, D_{k,x}^+ u_{i,j}^n, \\ D_{k,y}^- u_{i,j}^n, \dots, D_y^- u_{i,j}^n, D_y^+ u_{i,j}^n, \dots, D_{k,y}^+ u_{i,j}^n),$$

for a Lipschitz continuous function $h^A(x, y, p^-, p^+, q^-, q^+)$ (in short), with

$$D_{k,x}^\pm u_{i,j}^n := \pm \frac{u_{i,j\pm k}^n - u_{i,j}^n}{k\Delta x} \quad \text{and} \quad D_{k,y}^\pm u_{i,j}^n := \pm \frac{u_{i\pm k,j}^n - u_{i,j}^n}{k\Delta y}.$$

No assumptions on the stability of the high-order scheme are made.

Filter function

In our approach the *filter function* F must satisfy

- $F(r) \approx r$ for $|r| \leq 1$ so that if $|S^A - S^M| \leq \Delta t \varepsilon^n$ and $\phi_{i,j}^n = 1 \Rightarrow S^{AF} \approx S^A$
- $F(r) = 0$ for $|r| > 1$ so that if $|S^A - S^M| > \Delta t \varepsilon^n$ or $\phi_{i,j}^n = 0 \Rightarrow S^{AF} = S^M$

⇒ Several choices for F , different for regularity properties.

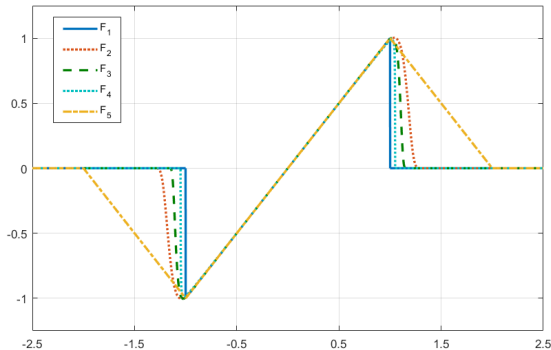


Figure: Possible choices for the filter function F .

Tuning of the parameter ε^n

If we want our scheme

$$u_{i,j}^{n+1} = S^{AF}(u^n)_{i,j} := S^M(u^n)_{i,j} + \phi_{i,j}^n \varepsilon^n \Delta t F \left(\frac{S^A(u^n)_{i,j} - S^M(u^n)_{i,j}}{\varepsilon^n \Delta t} \right),$$

to switch to the high-order scheme when some regularity is detected, we have to choose ε^n such that

$$\left| \frac{S^A(v^n)_{i,j} - S^M(v^n)_{i,j}}{\varepsilon^n \Delta t} \right| = \left| \frac{h^A(\cdot, \cdot) - h^M(\cdot, \cdot)}{\varepsilon^n} \right| \leq 1, \quad (11)$$

for $(\Delta t, \Delta x, \Delta y) \rightarrow 0$,

in the **region of regularity at time t_n**

$$\mathcal{R}^n := \{(x_j, y_i) : \phi_{i,j}^n = 1\}.$$

Smoothness indicator function

For the definition of a function ϕ , needed to detect the region \mathcal{R}^n , we require

$$\phi_{i,j}^n = \phi(\omega_{i,j}^n) := \begin{cases} 1 & \text{if the solution } u^n \text{ is regular in } I_{i,j}, \\ 0 & \text{if } I_{i,j} \text{ contains a point of singularity,} \end{cases}$$

where $I_{i,j} = [x_{j-1}, x_{j+1}] \times [y_{i-1}, y_{i+1}]$, ω_j^n is the *smoothness indicator at the node* x_j .

Remark

For $\varepsilon^n \equiv \varepsilon \Delta x$, with $\varepsilon > 0$ and $\phi_{i,j}^n \equiv 1$, we get the Basic Filtered Schemes of Bokanowski-Falcone-Sahu (2016), so we are generalizing that approach to exploit more carefully the local regularity of the solution at every time t_n and cell $I_{i,j}$.

\Rightarrow Under all these assumptions, the AF Scheme is convergent (See Falcone-Paolucci-T., Numerische Mathematik (2020), for details on the convergence theorem).

Smoothness indicator function

For the definition of a function ϕ , needed to detect the region \mathcal{R}^n , we require

$$\phi_{i,j}^n = \phi(\omega_{i,j}^n) := \begin{cases} 1 & \text{if the solution } u^n \text{ is regular in } I_{i,j}, \\ 0 & \text{if } I_{i,j} \text{ contains a point of singularity,} \end{cases}$$

where $I_{i,j} = [x_{j-1}, x_{j+1}] \times [y_{i-1}, y_{i+1}]$, ω_j^n is the *smoothness indicator at the node* x_j .

Remark

For $\varepsilon^n \equiv \varepsilon \Delta x$, with $\varepsilon > 0$ and $\phi_{i,j}^n \equiv 1$, we get the *Basic Filtered Schemes of Bokanowski-Falcone-Sahu (2016)*, so we are generalizing that approach to exploit more carefully the local regularity of the solution at every time t_n and cell $I_{i,j}$.

\Rightarrow Under all these assumptions, the AF Scheme is convergent (See Falcone-Paolucci-T., Numerische Mathematik (2020), for details on the convergence theorem).

Smoothness indicator function

For the definition of a function ϕ , needed to detect the region \mathcal{R}^n , we require

$$\phi_{i,j}^n = \phi(\omega_{i,j}^n) := \begin{cases} 1 & \text{if the solution } u^n \text{ is regular in } I_{i,j}, \\ 0 & \text{if } I_{i,j} \text{ contains a point of singularity,} \end{cases}$$

where $I_{i,j} = [x_{j-1}, x_{j+1}] \times [y_{i-1}, y_{i+1}]$, ω_j^n is the *smoothness indicator at the node* x_j .

Remark

For $\varepsilon^n \equiv \varepsilon \Delta x$, with $\varepsilon > 0$ and $\phi_{i,j}^n \equiv 1$, we get the *Basic Filtered Schemes of Bokanowski-Falcone-Sahu (2016)*, so we are generalizing that approach to exploit more carefully the local regularity of the solution at every time t_n and cell $I_{i,j}$.

⇒ Under all these assumptions, the AF Scheme is convergent (See Falcone-Paolucci-T., Numerische Mathematik (2020), for details on the convergence theorem).

Summary of Features/Advantages of the AF Scheme

- Several choices for F , different for regularity properties
- Several possible definition of the smoothness indicator function $\phi_{i,j}$
- Different coupling monotone/high-order schemes can be chosen (under some assumptions)
No assumptions on the stability of the high-order scheme are required!
- The AF scheme is convergent

Implementation details

We use the 2D version of the scheme S^{AF} by using Lax-Wendroff for S^A and Local Lax-Friedrichs for S^M .

Stopping Criterion: The iterations stop when the 0-level, or more precisely a neighborhood θ_δ of Γ_t of radius $\delta = \max\{\Delta x, \Delta y\}$, ceases to move.

$$E_\infty := \|u^{n+1} - u^n\|_{L^\infty(\theta_\delta)} = \max_{i,j} |F_{i,j}^n - F_{i,j}^{n-1}| < tol,$$

where $tol > 0$ is the prescribed tolerance. Another possible choice:

$$E_1 := \|u^{n+1} - u^n\|_{L^1(\theta_\delta)} = \Delta x \Delta y \sum_{i,j} |F_{i,j}^n - F_{i,j}^{n-1}| < tol(\Delta x, \Delta y),$$

where now the tolerance $tol > 0$ depends also on the discretization parameters.

Error Formulas:

$$P\text{-err}_{rel} = \frac{|N_e - N_a|}{N_e}, \quad P\text{-err}_1 = |N_e - N_a| \Delta x \Delta y$$

where

$N_e = \#$ pixels of the exact object

$N_a = \#$ pixels of the approximated object via the chosen scheme.

Synthetic Rhombus - Expansion case

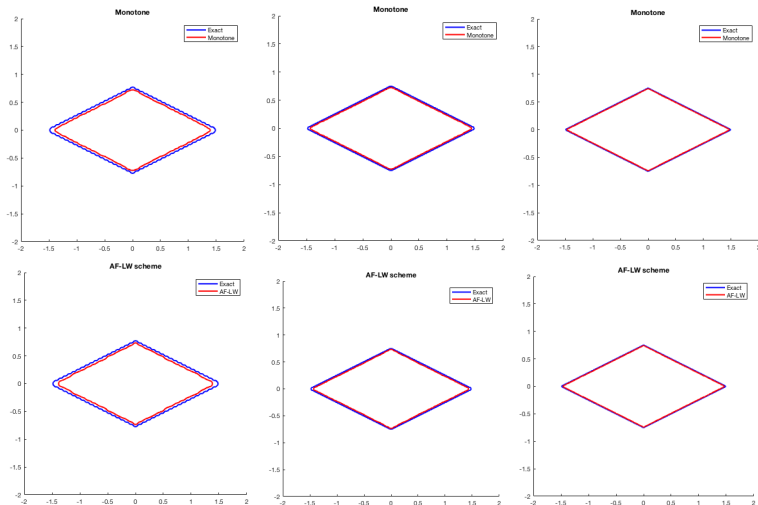


Figure: Plots of the final front obtained by the Monotone scheme (top) and the AF-LW scheme (bottom) with $tol = 0.0005$, $\mu = 2$, $K_{reg} = 0$, and velocity \tilde{c} .

Synthetic Rhombus - Expansion case

Table: Errors and number of iterations using L^∞ norm varying $\#Nodes$. $tol = 0.0005$, $\mu = 2$, $K_{reg} = 0$.

c	Monotone			AF-LW			WENO		
$\#Nodes$	N_i	$P-Err_{rel}$	$P-Err_1$	N_i	$P-Err_{rel}$	$P-Err_1$	N_i	$P-Err_{rel}$	$P-Err_1$
102	84	0.1025	0.2321	213	X	X	217	X	X
202	152	0.0526	0.1172	394	X	X	399	X	X
402	288	0.0265	0.0593	745	X	X	669	X	X

Table: Errors and number of iterations using L^∞ norm varying $\#Nodes$. $tol = 0.0005$, $\mu = 2$, $K_{reg} = 0$.

\tilde{c}	Monotone			AF-LW			WENO		
$\#Nodes$	N_i	$P-Err_{rel}$	$P-Err_1$	N_i	$P-Err_{rel}$	$P-Err_1$	N_i	$P-Err_{rel}$	$P-Err_1$
102	50	0.0748	0.1694	48	0.0693	0.1568	47	0.0886	0.2008
202	100	0.0427	0.0950	96	0.0363	0.0808	96	0.0469	0.1045
402	199	0.0208	0.0466	196	0.0203	0.0454	196	0.0240	0.0537

Geometric Shapes - Shrinking case

Initial front

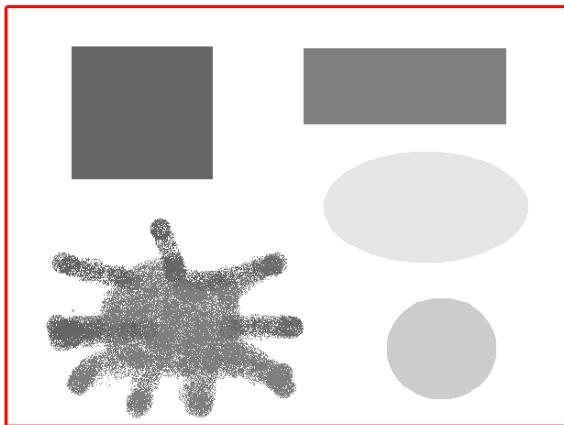


Figure: Initial front for the shrinking case.

Geometric Shapes - Shrinking case

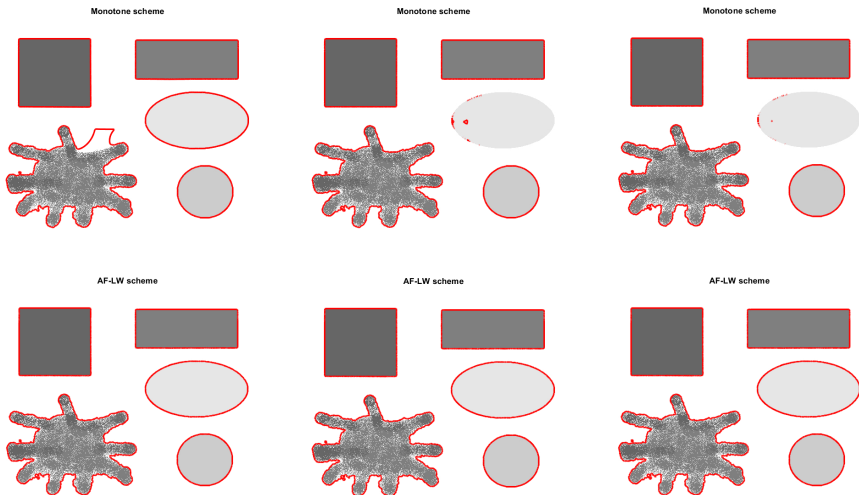
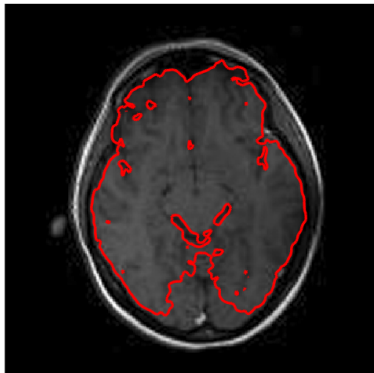


Figure: Plots of the final front using the monotone scheme (top), and the AF-LW scheme (bottom) varying the tolerance ($tol = 0.0005, 0.0001, 0.00005$) with $\mu = 4$, $K_{reg} = 1$, and velocity \tilde{c} .

Real Brain - Expansion case

Monotone scheme



AF-LW scheme

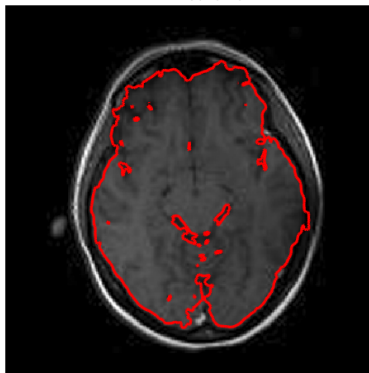


Figure: Plots of the final front using the monotone scheme, $N_i = 376$ (left), and the AF-LW scheme, $N_i = 407$ (right), all using L^1 norm in the stopping criterion and $tol = 0.00001$, $\mu = 4$ and $K_{reg} = 5$, and velocity \tilde{c} .

Real Brain - Shrinking case

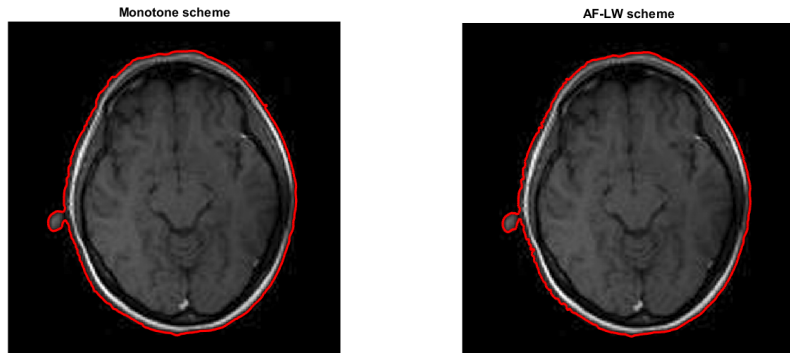
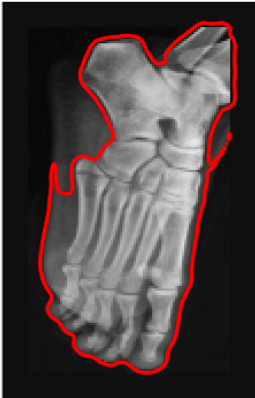


Figure: Plots of the final front using the monotone scheme (left) and the AF-LW scheme (right) with velocity \tilde{c} .

\tilde{c}, L^1	Monotone				AF-LW			
	N_i	(sec.)	$P-Err_{rel}$	$P-Err_1$	N_i	(sec.)	$P-Err_{rel}$	$P-Err_1$
170×170	83	0.80	0.0465	0.2436	87	3.75	0.0439	0.2300
340×340	228	8.39	0.0118	0.2476	262	46.07	0.0078	0.1628

Real foot fracture - Shrinking case

Monotone scheme



AF-LW scheme



Figure: Plots of the final front using the monotone scheme ($N_i = 156$), and the AF-LW scheme ($N_i = 243$), with L^1 norm and $tol = 0.00005$, $\mu = 4$, $K_{reg} = 5$, $\Delta x = 0.02$ and velocity \tilde{c} .

Real Pneumonia - Expansion case

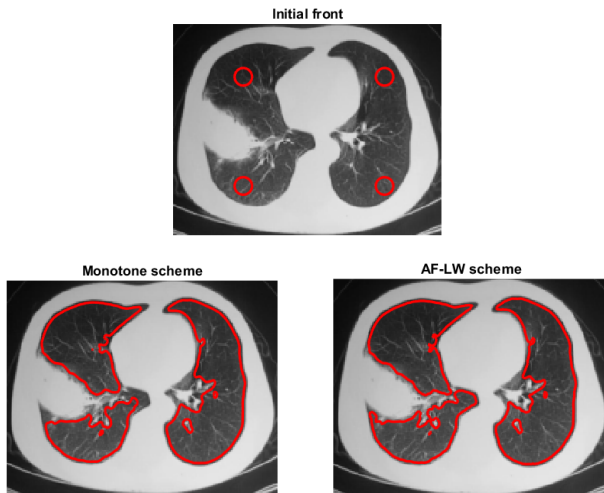


Figure: Plots of the final front using the monotone scheme ($N_i = 185$), and the AF-LW scheme ($N_i = 194$), with L^1 norm and $tol = 0.00001$, $\mu = 4$, $K_{reg} = 5$, and velocity \tilde{c} .








Conclusions - Stationary Part

- 1 We approximate viscosity solutions
- 2 Well-posedness of the Orthographic PS-SfS problem using 2 images + BCs or 3 images without boundary conditions for a generic surface
- 3 We need only one or two input images for some special cases (4 or 1 axes of symmetry, respectively)
- 4 Non-Lambertian reflectance models do not solve the ambiguity, but can improve results







Conclusions - Evolutive Part

- 1 We presented a rather simple way to construct convergent schemes, which are of high-order in regions of regularity.
- 2 Our procedure is able to stabilize an otherwise unstable (high-order) scheme, still preserving its accuracy.
- 3 We define new 2D smoothness indicators, applying them in the construction of AF schemes.
- 4 The adaptive filtered scheme can be used efficacily and in a easily way to solve the image segmentation problem.
- 5 We noticed that the new velocity function \tilde{c} introduced in the LS model can improve a lot the results, especially for biomedical images.

References - Stationary Part







-  J.-D. Durou, M. Falcone, Y. Quéau, **S. Tozza** (Eds.), *Advances in Photometric 3D-Reconstruction*, ACVPR Series, Springer 2020.
-  **S. Tozza**, M. Falcone, Analysis and approximation of some Shape-from-Shading models for non-Lambertian surfaces, *JMIV*, **55**(2):153-178, 2016.
-  R. Mecca, M. Falcone, Uniqueness and approximation of a Photometric Shape-from-Shading model, *SIAM J. Imaging Sciences*, **6**(1):616-659, 2013.
-  **S. Tozza**, R. Mecca, M. Duocastella, A. Del Bue, Direct Differential Photometric Stereo Shape Recovery of Diffuse and Specular Surfaces, *JMIV*, **56**(1):57-76, 2016.
-  R. Mecca, **S. Tozza**, Shape Reconstruction of Symmetric Surfaces using Photometric Stereo, In: *Innovations for Shape Analysis: Models and Algorithms*, pp. 219-243, Springer Edition, 2013.
-  F. Camilli, **S. Tozza**, A Unified Approach to the Well-Posedness of Some Non-Lambertian Models in Shape-from-Shading Theory, *SIAM J. Imaging Sci.* , **10**:26–46, 2017.
-  **S. Tozza**, Perspective Shape-from-Shading Problem: A Unified Convergence Result for Several Non-Lambertian Models, *J. Imaging*. **8**, 36, 2022.

References - Evolutive Part

-  O. Bokanowski, M. Falcone, S. Sahu, An efficient filtered scheme for some first order Hamilton-Jacobi-Bellman equations, *SIAM Journal on Scientific Computing*, **38**(1):A171–A195, 2016.
-  M. Falcone, G. Paolucci, **S. Tozza**, Convergence of Adaptive Filtered schemes for first order evolutionary Hamilton-Jacobi equations, *Numerische Mathematik*, **145**(2):271–311, 2020
-  M. Falcone, G. Paolucci, **S. Tozza**, A High-Order Scheme for Image Segmentation via a modified Level-Set method, *SIAM J. Imaging Sci.*, **13**(1): 497–534, 2020
-  M. Falcone, G. Paolucci, **S. Tozza**, Multidimensional smoothness indicators for first-order Hamilton-Jacobi equations, *Journal of Computational Physics*, 2020
-  R. Malladi, J. A. Sethian, B. C. Vemuri, *Shape modeling with front propagation: A level set approach*, Center for Pure and Applied Mathematics, Report PAM-589, Univ. of California, Berkeley, August 1993.
-  A.M. Oberman and T. Salvador, Filtered schemes for Hamilton-Jacobi equations: a simple construction of convergent accurate difference schemes, *Journal of Computational Physics*, **284**:367–388, 2015

THANK YOU FOR YOUR ATTENTION!

References - Evolutive Part

-  O. Bokanowski, M. Falcone, S. Sahu, An efficient filtered scheme for some first order Hamilton-Jacobi-Bellman equations, *SIAM Journal on Scientific Computing*, **38**(1):A171–A195, 2016.
-  M. Falcone, G. Paolucci, **S. Tozza**, Convergence of Adaptive Filtered schemes for first order evolutionary Hamilton-Jacobi equations, *Numerische Mathematik*, **145**(2):271–311, 2020
-  M. Falcone, G. Paolucci, **S. Tozza**, A High-Order Scheme for Image Segmentation via a modified Level-Set method, *SIAM J. Imaging Sci.*, **13**(1): 497–534, 2020
-  M. Falcone, G. Paolucci, **S. Tozza**, Multidimensional smoothness indicators for first-order Hamilton-Jacobi equations, *Journal of Computational Physics*, 2020
-  R. Malladi, J. A. Sethian, B. C. Vemuri, *Shape modeling with front propagation: A level set approach*, Center for Pure and Applied Mathematics, Report PAM-589, Univ. of California, Berkeley, August 1993.
-  A.M. Oberman and T. Salvador, Filtered schemes for Hamilton-Jacobi equations: a simple construction of convergent accurate difference schemes, *Journal of Computational Physics*, **284**:367–388, 2015

THANK YOU FOR YOUR ATTENTION!

Ciao Maurizio, Thanks for all! We miss you very much...

